

Received April 21, 2021, accepted May 4, 2021, date of publication May 10, 2021, date of current version May 18, 2021.

Digital Object Identifier 10.1109/ACCESS.2021.3078768

Finite-Time Sliding Mode Control With Unknown Control Direction

DONGMEI LÜ 

Anhui Communications Vocational and Technical College, Hefei 230051, China

e-mail: kanzhen0322@gmail.com

This work was supported in part by the Natural Science Research Project of Anhui University: Research on Fault Monitoring and Dynamic Characteristics of Spindle System in Machining Center under Grant KJ2020A1060, and in part by the Anhui Quality Engineering Project: Electromechanical Integration Technology Specialty Group of Anhui Communications Vocational and Technical College under Grant 2020zyq25.

ABSTRACT In this paper, a global nonsingular sliding mode controller is developed for a second order system with unknown control direction. A novel terminal sliding mode hypersurface is presented to compensate for the sign uncertainty in the control input and avoid the singularity issue present in the traditional terminal sliding mode control. In contrast to the Nussbaum gain approach where the equilibrium point is reached asymptotically in the presence of input sign uncertainty, the proposed controller guarantees that the equilibrium point can be reached from any initial state in finite time. Simulation results are provided to validate the proposed controller.


INDEX TERMS Finite-time sliding mode control, unknown control direction.

I. INTRODUCTION

Sliding mode control (SMC) is a well known control technique due to its insensitivity to parameter variations and exogenous disturbances [1]. The crucial aspect of SMC is in the sliding surface design that restricts the motion of the system states to a sliding manifold. Typically, the system states converge to an equilibrium point asymptotically or exponentially using linear surface design. Approaches using terminal sliding mode (TSM) offers finite time convergence and superior performance compared to linear sliding surfaces [2]–[6]. Although TSM has been widely accepted due to finite time convergence for systems with model uncertainties and disturbances, the existing TSM solutions do not take into account the unknown control direction, i.e., the sign uncertainty in the input matrix. The input sign uncertainty may arise in scenarios such as when a control signal is sent to a system over an unassured and possibly hostile communication channel and even due to manufacturing defects when a large number of systems (e.g., quadrotors) are manufactured in batches [7]. This work is particularly motivated to consider sliding mode control of systems with input sign uncertainties.

The challenges in control design due to input sign uncertainty have led to some creative ways to circumvent the problem. One of the widely used techniques employs

Nussbaum-type gain functions to compensate for the sign uncertainty. In [8], the Nussbaum and reference type functions were used to design a global adaptive controller for an n -order system. In [9], Yang *et al.* divided the state into convergent and non-convergent sets to analyze the Nussbaum gain when the sign switching occurs in the intervals between the switchings. Learning-based control methods are also used in conjunction with Nussbaum functions to compensate for the lack of knowledge in the control direction [10], [11]. Recently, Nussbaum function is used in consensus of multi-agent systems with unknown control direction [7], [12]. A practical application is addressed in [13] for hypersonic missiles, when the transformed system yield unknown control direction due to uncertainty in the original dynamics. However, Nussbaum-based controllers can only guarantee asymptotic convergence and exhibit peaking phenomenon due to the high-gain feature of these controllers [14], [15], which may pose practical challenges. Apart from the Nussbaum-type gain, monitoring functions have also been used to detect sign changes in the control direction [16], [17]. In [18], the monitoring function is used to overcome uncertainties in camera orientation angle. In [19], Scheinker and Krstić designed minimum seeking control Lyapunov functions for the systems with unknown control direction. Other representative works include fuzzy adaptive control [20], Nussbaum-based control for actuator failures [21], and adaptive neural control [22].

The associate editor coordinating the review of this manuscript and approving it for publication was Haibin Sun .

Robust control methods are alternatives to compensate for the unknown control direction. In [23], a continuous robust controller with an online algorithm to identify changes in the control direction is designed to guarantee uniformly ultimately bounded stability in the presence of unknown time-varying control direction. In [15], Bartolini *et al.* used SMC to compensate for the sign of the input matrix with an observer designed to estimate the drift terms to ensure asymptotic stability of the origin. In [24], Bartolini *et al.* designed a so called “suboptimal” second order sliding mode control algorithm in the presence of constant unknown control direction. Drakunov *et al.* divided the system state space into cells with smooth boundaries [25]. The inside of each of these cells contains a fixed control direction. The control direction alternates between the cells, which results in a set of stability points where the input matrix is nonsingular. In contrast to standard SMC where the sliding mode occurs when the sliding surface is near zero, this method allows the sliding motion to occur when the sliding surface is at a constant. The sliding surface can be driven to origin by removing the steady state error using dynamic compensator. The controller design in [25] is based on periodic switching function and the fact that the cells have smooth sliding manifolds as their boundaries. Although it allows the system to go from one manifold to another reaching the equilibrium point, it only yields local stability result.

The contribution of this paper is multifold. First, compared to the work of [26], the sliding surface design is nonsingular, and there is no singularity as the state reaches the origin in the presence of unknown control direction. Second, leveraging on the works of [25] and [27], the sliding surface design allows the control input to remain bounded, yielding globally finite time result. Third, this work considers time-varying unknown control direction. As opposed to Nussbaum-based controllers (e.g., in [8], [28], [29]) that yield asymptotic stability, and the super-twisting control algorithm in [30] that only guarantees exponential stability, the controller in this paper guarantees *finite time* convergence of the system states to the origin in the presence of non-vanishing disturbance. In addition, the developed controller compensates for unknown non-vanishing state-dependent exogenous disturbances and unknown time-varying control direction. The presented controller does not employ logic tests [15], [24], [31], [32] or monitoring functions [16] to determine the hard uncertainty in the control input. Simulations results are provided to validate the effectiveness of the proposed control structure.

II. BACKGROUND

The basic principles of finite time convergence and controller design in the presence of unknown control direction, used in this paper, can be briefly summarized in the lemmas given below.

Lemma 1 [6]: Consider the first order system given as $\dot{x} = -\beta x^{\gamma_1/\gamma_2}$, where $\beta \in \mathbb{R}^+$, $0 < \gamma_1/\gamma_2 < 1$, γ_1 and γ_2 are odd integers. The state $x(t) \rightarrow 0$ in finite time.

Lemma 2 [27]: Let the first order system be given by

$$\dot{x} = f(x, t) + bu(t)$$

where $f(x, t) \in \mathbb{R}$ is the disturbance, $b \in \mathbb{R}$ is the input gain with unknown sign, and the control input $u(t)$ is designed as

$$u = M \operatorname{sgn}\left(\sin \frac{\pi}{\varepsilon} \tilde{s}\right)$$

where $\operatorname{sgn}(\cdot)$ denotes the sign of (\cdot) , $\varepsilon \in \mathbb{R}^+$ is a constant, $M \in \mathbb{R}^+$ is a constant or a positive function, and the hypersurface $\tilde{s}(t)$ is defined as

$$\tilde{s} = s + \lambda \int \operatorname{sgn}(s)dt$$

with $s(t) = x(t)$ as the sliding surface and $\lambda \in \mathbb{R}^+$. When the gain M is designed to satisfy the inequality $|Mb| > |f| + \lambda$, the surface $s(t) \rightarrow 0$ in finite time.

III. PROBLEM FORMULATION

Consider an uncertain system modeled as a double integrator and subjected to nonvanishing disturbances as

$$\begin{aligned} \dot{x}_1 &= x_2 \\ \dot{x}_2 &= f(x, t) + b(x, t)u \end{aligned} \tag{1}$$

where $x_1(t), x_2(t) \in \mathbb{R}$ are the states and let $x = [x_1 \ x_2]^T$, $b = b(x, t) \in \mathbb{R}$ be the control gain with unknown sign, $f(x, t) \in \mathbb{R}$ is the nonvanishing disturbance, and $u(t) \in \mathbb{R}$ is the control input.

Assumption 1 [15]: The nonvanishing disturbance $f(x, t)$ is upper bounded by a constant $\bar{f} \in \mathbb{R}^+$ as

$$|f(x, t)| \leq \bar{f} \quad \forall(x, t).$$

Assumption 2 [30]: The control gain $b(x, t)$ can be bounded as $\underline{b} \leq |b(x, t)| \leq \bar{b}$, where $\underline{b}, \bar{b} \in \mathbb{R}^+$. The sign of $b(x, t)$ is unknown, i.e., the control direction is unknown.

Assumption 3 [33]: The rate of sign changes of $b(x, t)$ is slow.

To facilitate the subsequent analysis, four quadrants $Q_i \forall i = 1, 2, 3, 4$ are defined using the following inequalities:

$$\begin{aligned} Q_1: \{x_1 \geq 0, x_2 \geq 0\} & \quad Q_2: \{x_1 < 0, x_2 > 0\} \\ Q_3: \{x_1 \leq 0, x_2 \leq 0\} & \quad Q_4: \{x_1 > 0, x_2 < 0\} \end{aligned}$$

The objective of this paper is to design a robust controller that ensures finite time convergence of the system in (1) in the presence of sign uncertainty in the control input and nonvanishing disturbances.

IV. SLIDING SURFACE DESIGN

Based on the nonsingular terminal sliding mode control in [6], the surface $s(t)$ can be modified as

$$s = e^{c_2 x_2^2/2} x_2^{m_2/m_1} + c x_1 \tag{2}$$

where $m_1, m_2 \in \mathbb{Z}^+$ are odd integers, $1 < m_2/m_1 < 2$, $(m_2 + m_1)/m_1 > 1$, $(m_2 - m_1)/m_1 < 1$, and $c, c_2 \in \mathbb{R}^+$ are constants. When $s = 0 : x_2 = (-c x_1)^{m_1/m_2} e^{-m_1 c_2 x_2^2/(2m_2)}$,

x_1 and x_2 go to the equilibrium point in finite time. To compensate for the sign uncertainty in b , the augmented sliding surface $\tilde{s}(t)$ is designed as

$$\tilde{s} = s + \lambda \int \sigma^{p_1/p_2}(s(\tau))d\tau \quad (3)$$

where $\lambda \in \mathbb{R}^+$ is a constant, $p_1, p_2 \in \mathbb{Z}^+$ are odd integers that satisfy $0 < p_1/p_2 < 1$, and $\sigma(s)$ is a saturation function with the maximum magnitude of $M_s \in \mathbb{R}^+$ and $\sigma(s) = s(t)$ for $|s(t)| \leq L_s \in \mathbb{R}^+$. The constants L_s, M_s are designed parameters chosen based on the user requirements. Taking time derivative of (2) and (3) along (1), the rate of change of the surfaces $s(t)$ and $\tilde{s}(t)$ can be obtained as

$$\dot{s} = g\dot{x}_2 + cx_2 \quad (4)$$

$$\dot{\tilde{s}} = \dot{s} + \lambda\sigma^{p_1/p_2}(s) \quad (5)$$

$$g = \left(c_2x_2^{(m_1+m_2)/m_1} + \frac{m_2}{m_1}x_2^{(m_2-m_1)/m_1} \right) e^{c_2x_2^2/2} \quad (6)$$

where $g(x) \in \mathbb{R}$ is a positive semi-definite function due to the fact that $m_2 + m_1$ and $m_2 - m_1$ yield even integers. Substituting (1) and (4) into (5), the open-loop system can be expressed as

$$\dot{\tilde{s}} = g(f + bu) + cx_2 + \lambda\sigma^{p_1/p_2}(s). \quad (7)$$

The surface in $\tilde{s}(t)$ is partitioned into four parts, and the control is designed to compensate for each of the terms in (7).

Remark 1: The sliding surface in (2) is different from the classical nonsingular terminal sliding surface. The function $e^{c_2x_2^2/2}$ in (2) behaves similar to a saturation function of $x_1(t)$ without the nonsmooth derivative at the boundary in the sense that it increases the magnitude of $e^{c_2x_2^2/2}x_2^{m_2/m_1}$ to dominate cx_1 . Thus, the surface $s(t)$ in (2) has the benefit of allowing the control gain in $u(t)$ to be multiplied by the function $g(x_2)$ in (7) to be larger than the terms $\lambda\sigma^{p_1/p_2}(s)$ and cx_2 without the need to increase the magnitude of $u(t)$. This is significant in the sense that it aids the system in (1) to slide on the surface $\tilde{s}(t)$ and enables global finite time stability rather than local stability as in [27]. This will become clear in the subsequent analysis.

V. CONTROLLER DEVELOPMENT

To facilitate the subsequent analysis, the control input $u(t)$ in (1) is segregated into four terms as

$$u = u_1 + u_2 + u_3 + u_4, \quad (8)$$

which are designed separately in (14)-(17). Substituting (8) into (7), the open-loop error dynamics can also be subdivided into four parts

$$\dot{\tilde{s}} = P_1(x) + P_2(x) + P_3(x) + P_4(x) \quad (9)$$

where the functions $P_1(x), P_2(x), P_3(x), P_4(x) \in \mathbb{R}$ are given as

$$P_1(x) = gbu_1 + cx_2 \quad (10)$$

$$P_2(x) = g(f + bu_2) \quad (11)$$

$$P_3(x) = gbu_3 + \lambda\sigma^{p_1/p_2}(s) \quad (12)$$

$$P_4(x) = gbu_4. \quad (13)$$

For notational simplicity, consider the auxiliary functions $\Psi(\tilde{s})$ and $\Psi_s(\tilde{s})$ defined as

$$\Psi \triangleq \text{sgn} \left(\sin \frac{\pi}{\varepsilon} \tilde{s} \right) \quad \Psi_s \triangleq \text{sgn}(b\Psi)$$

where $\varepsilon \in \mathbb{R}^+$ is the constant spacing between manifolds $\tilde{s}(t)$.

Based on the subsequent analysis, the control input $u(t)$ can be designed as

$$u_1 = M_1\Psi \quad (14)$$

$$u_2 = M_2\Psi \quad (15)$$

$$u_3 = |\sigma(s)|^{p_1/p_2}M_3\Psi. \quad (16)$$

$$u_4 = \frac{m_1}{m_2}|\sigma(s)|^{q_1/q_2}M_4\Psi \quad (17)$$

where $M_1, M_2, M_3, M_4, q_1, q_2 \in \mathbb{R}^+$ are constants. Substituting (14)-(17) into (7), the closed-loop system can be expressed as

$$\begin{aligned} \dot{\tilde{s}} = & gbM_1\Psi + cx_2 + g(f + bM_2\Psi) + gb|\sigma(s)|^{p_1/p_2}M_3\Psi \\ & + gb\frac{m_1}{m_2}|\sigma(s)|^{q_1/q_2}M_4\Psi + \lambda\sigma^{p_1/p_2}(s). \end{aligned} \quad (18)$$

The following lemmas demonstrate the magnitude of the control input $u(t)$ dominates the disturbance and the terms that are not canceled due to the unknown control direction. Each lemma addresses the control design in (14)-(17) such that $\Psi(\tilde{s})$ is dominant in (10)-(13). According to [6] and [27], when the terms containing $\Psi(\tilde{s})$ dominate the expression in (18), sliding mode occurs and $\Psi(t)$ converges to a constant, resulting in that $s(t), x(t) \rightarrow 0$ in finite time.

Lemma 3: The control input $u_1(t)$ and $u_2(t)$ designed in (14) and (15), respectively, allow the sign of $\Psi(\tilde{s})$ to dominate in (10) and (11).

Proof: The proof is in Appendix A. ■

In (12), as $x_2(t) \rightarrow 0$, the function $g(x_2)$ also decreases, which causes the magnitude of $u_3(t)$ unable to dominate in (12). The following Lemma finds the region where $g(x_2)$ is large enough to help $u_3(t)$ dominate in (12). As $x_2(t) \rightarrow 0$, there must be a value of $x_2(t)$ where $|x_2(t)| = x_{2m} \in \mathbb{R}^+$ such that the magnitude of $|gbu_3| = \lambda M_s^{p_1/p_2}$. When $|x_2| \geq x_{2m}$, $|gbu_3| \geq \lambda M_s^{p_1/p_2}$ and sliding mode occurs. The following Lemma summarizes the above discussion.

Lemma 4: Define the set $x_{2a} \subset \mathbb{R}$ as

$$x_{2a} = \left\{ x_2 \mid g(x_2) - \frac{\lambda M_s}{bM_3} = 0, x_2 \neq 0 \right\} \quad (19)$$

where $g(x_2)$ is defined in (6). For the region defined by $|s(t)| > L_s$ and $|x_2(t)| \geq x_{2m}$, the sign of Ψ_s is dominant in $P_3(x)$, where x_{2m} can be defined as

$$x_{2m} \triangleq \text{maxima}(x_{2a}), \quad (20)$$

and it can be selected by varying control gain M_3 .

Proof: The proof is in Appendix B. ■

To facilitate the controller development, four regions \mathcal{R}_i for $i = 1, 2, 3, 4$ are defined as

$$\begin{aligned} \mathcal{R}_1 &\triangleq \{(x_2, s) \mid |x_2| < x_{2m}, |s| > L_s\} \\ \mathcal{R}_2 &\triangleq \{(x_2, s) \mid |x_2| \leq x_{2m}, |s| \leq L_s\} \\ \mathcal{R}_3 &\triangleq \{x_2 \mid |x_2| \leq x_{2m}\} \\ \mathcal{R}_4 &\triangleq \{x_2 \mid |x_2| > x_{2m}\}. \end{aligned}$$

It can be seen that $\mathcal{R}_2 \subset \mathcal{R}_3$, and \mathcal{R}_2 contains the origin of (1). Using the definition of the surface $s(t)$ in (2), the set \mathcal{R}_2 implies that $|e^{c_2 x_{2m}^2/2} x_{2m}^{m_2/m_1} + c x_1| \leq L_s$.

Figure 1 shows the boundary x_{2m} defined in (20), such that $\mathcal{R}_4 \subset \mathbb{R}^2$ is defined to be the region outside the green lines, i.e., $|x_2(t)| > x_{2m}$. Consider the case when $x(t) \in \mathcal{Q}_1 \cap \mathcal{R}_4$ and suppose sliding mode has not occurred, and the control input $u(t)$ causes $x_2(t)$ to increase. Using (1) and the fact that $x_2(t) > 0$ in $x(t) \in \mathcal{Q}_1 \cap \mathcal{R}_4$, $x_1(t)$ increases monotonically. However, since $x_2(t) \in \mathcal{R}_4$, according to Lemmas 3 and 4, the terms containing $\Psi(\tilde{s})$ dominate in (9), and $x(t)$ is attracted to one of the manifolds $\tilde{s}(t) = \beta$, where $\beta \in \mathbb{R}$, in finite time. Therefore, from (1) and (2), $|x_2(t)|$ decreases until $x_2(t)$ enters the region \mathcal{R}_3 . Similar arguments can be made when $x(t) \in \mathcal{Q}_3 \cap \mathcal{R}_4$ to show that $x_2(t)$ starts in \mathcal{R}_4 and enters \mathcal{R}_3 .

Figure 1 and Figure 2 show the direction of $bu(t)$ with respect to the sliding manifold $\tilde{s} = \beta = k\varepsilon$ for $k = \pm 1, \pm 3, \pm 5, \dots$. As shown in Figure 2, $\Psi_s = +1$ is on the left and $\Psi_s = -1$ is on the right of $\tilde{s} = \beta$.

From (7), as $x_2(t)$ approaches zero, the function $g(x_2)$ also approaches zero. Since the control input $u(t)$ is multiplied by $g(x_2)$ in (7), the surface $\tilde{s}(t)$ becomes uncontrollable when $g(x_2) = 0$ and (x_1, x_2) can get stuck in \mathcal{R}_1 . The following lemma addresses this issue by proving that the line $x_2 = 0$

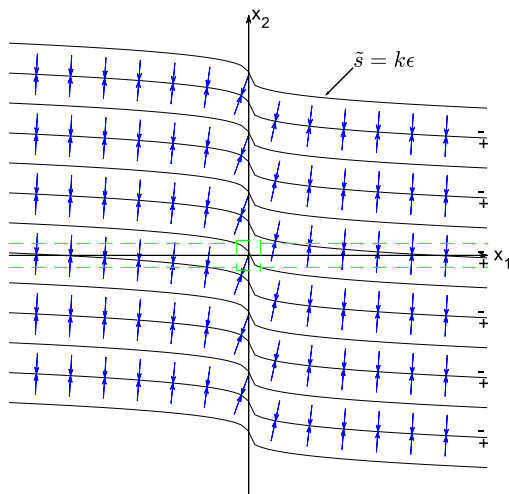


FIGURE 1. Multiple equilibrium surface $\tilde{s} = k\varepsilon$, and the boundary x_{2m} shown in dotted green line. '+' and '-' represent the signs of $bu(t)$ such that \uparrow indicates $\text{sgn}(bu) = +1$ and \downarrow indicates $\text{sgn}(bu) = -1$ for the control input acting on \tilde{s} .

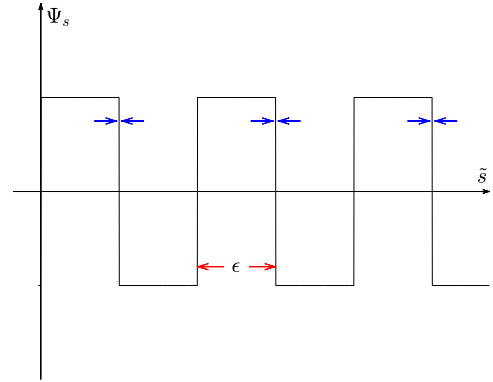


FIGURE 2. Plot of $\Psi_s(t)$ showing $\Psi_s = +1$ on the left and $\Psi_s = -1$ on the right with respect to a sliding manifold $\tilde{s} = \beta = k\varepsilon$ for $k = \pm 1, \pm 3, \pm 5, \dots$. The arrow \rightarrow indicates $\text{sgn}(bu) = +1$ and \leftarrow indicates $\text{sgn}(bu) = -1$.

and the set $x_2(t) \in \mathcal{R}_1$ is an unattractive set, i.e., (x_1, x_2) does not get stuck at $x_1 \neq 0$ and $x_2 = 0$. In fact, the following lemma demonstrates that (x_1, x_2) escapes the neighborhood of $x_2 = 0$ in finite.

Lemma 5: Let the sliding mode occur before $x(t)$ enters \mathcal{R}_3 , and let $x_2(t)$ enter \mathcal{R}_3 with $\Psi_s = -1$ and $|s(t)| > L_s$. When M_3 is designed to satisfy the inequality

$$M_3 > \frac{4x_{2m}}{\underline{b}(\varepsilon - 2M_s^{p_1/p_2} \varepsilon_{\tilde{s}})} \quad (21)$$

$x_2(t)$ leaves \mathcal{R}_3 and enters \mathcal{R}_4 in finite time, where $\varepsilon_{\tilde{s}} \in \mathbb{R}^+$.

Proof: The proof is in Appendix C. ■

In Lemma 5, $x_2(t)$ can also enter \mathcal{R}_3 with $\Psi_s = +1$, and let $s(t)$ be positive. Since $\text{sgn}(s) = \text{sgn}(\Psi_s)$, the function $\sigma^{p_1/p_2}(s)$ is an aiding term, forcing the state $x(t)$ to be attractive to the manifold $\tilde{s}(t) = \beta$. This pushes $x(t)$ to the other side of the manifold with $\Psi_s = -1$, where sliding mode no longer occurs because $|\dot{\tilde{s}}| < \lambda \sigma^{p_1/p_2}(s)$ and the terms containing Ψ_s no longer dominate in (29). Thereafter, Lemma 5 can be used to conclude that $x_2(t)$ leaves \mathcal{R}_3 .

Similar to [6], Lemma 5 above proves that $x_2(t)$ crosses the boundary layer $|x_2| \leq x_{2m}$, which includes $x_2 = 0$. If the initial conditions are $x_2(t) = 0$ and $\Psi_s = 0$ with $s(t) \neq 0$, then the surface in (7) is not zero, and, by definition, Ψ_s will change to ± 1 . Then, the velocity $x_2(t)$, in the worst case scenario, leaves \mathcal{R}_3 , attaches itself to a sliding manifold and re-enters \mathcal{R}_3 . Once $x_2(t) \in \mathcal{R}_3$, using Lemmas 3-5, it can be shown that the velocity crosses the boundary layer $|x_2| \leq x_{2m}$ in finite time, and $|x_2| \leq x_{2m}$ is not an attractive set.

As $x_2(t)$ leaves the boundary layer $|x_2(t)| \leq x_{2m}$ and the magnitude of $x_2(t)$ increases, $x_1(t)$ approaches the origin and $x_2(t)$ approaches a constant. The following lemma illustrates this point.

Lemma 6: Let the sliding mode occur on $\tilde{s}(t) = \beta$, $|s(t)| > L_s$, $x_2(t) \in \mathcal{R}_4$, and $x(t) \in \mathcal{Q}_2$ or $x(t) \in \mathcal{Q}_4$, then $x_1(t)$ approaches the origin with an average constant velocity of $x_{2\text{avg}} = -\lambda M_s^{p_1/p_2} \text{sgn}(s)/c$.

Proof: The proof is in Appendix D. ■

Lemmas 3-5 show that sliding mode occurs in \mathcal{R}_4 and $x_2(t)$ enters and exits \mathcal{R}_3 from \mathcal{Q}_1 to \mathcal{Q}_4 or from \mathcal{Q}_3 to \mathcal{Q}_2 . However, for $x(t)$ to reach the origin in finite time, sliding mode must also occur in \mathcal{R}_2 . If sliding mode does not occur as $x_2(t)$ enters \mathcal{R}_2 , then $x(t)$ is not attached to a manifold. If this is the case, then $x_2(t)$ either stays in \mathcal{R}_2 or exits \mathcal{R}_2 until it attaches itself to an attractive manifold. The following lemma demonstrates that when sliding mode occurs as $x_2(t)$ enters \mathcal{R}_2 then sliding mode continues to occur for $x_2(t) \in \mathcal{R}_2$.

The need for the following lemma is motivated by the fact that the magnitude of the term $g(x_2)bu(t)$ in (7) has to be larger than $\lambda\sigma^{p_1/p_2}(s)$ in order for sliding mode to occur. Since the control input scalar $b(x, t)$ is uncertain, exactly cancellation of $\sigma^{p_1/p_2}(s)$ is not possible, thus, it is desirable to design the hypersurface in (7) such that $\lambda|\sigma^{p_1/p_2}(s)|$ is smaller than $|g(x_2)bu(t)|$. The lemma below establishes inequalities that force $\lambda|\sigma^{p_1/p_2}(s)|$ to be smaller than $|g(x_2)bu(t)|$ as $\tilde{s}(t) \rightarrow 0$.

Lemma 7: When sliding mode occurs as $x(t)$ enters \mathcal{R}_2 , the control input $u_4(t)$ designed in (17) allows the sign of Ψ_s to be dominant in (29) and sliding mode continues to occur in \mathcal{R}_2 .

Proof: The proof is in Appendix E. ■

From (1), when sliding mode occurs on one of the manifolds in \mathcal{Q}_2 or \mathcal{Q}_4 , it is possible that $x(t)$ stays in \mathcal{Q}_2 or \mathcal{Q}_4 , respectively, while converging to the origin. Additional analysis for $x(t) \in \mathcal{Q}_2$ and $x(t) \in \mathcal{Q}_4$ is trivial if $x(t)$ remains in \mathcal{Q}_2 or \mathcal{Q}_4 until $x(t)$ reaches the origin since, according to Lemma 6, $x_2(t)$ will not enter \mathcal{R}_3 until it reaches \mathcal{R}_2 . If the initial velocity $x_2(t_0)$ is in \mathcal{Q}_2 or \mathcal{Q}_4 and crosses over to \mathcal{Q}_1 or \mathcal{Q}_3 , respectively, then Lemma 3-7 can be used to show finite time convergence of $x(t)$. Moreover, from Lemma 6, once sliding mode occurs in \mathcal{Q}_2 or \mathcal{Q}_4 , the velocity $x_2(t)$ approaches the origin with an average velocity of $x_{2avg} = -\lambda M_s^{p_1/p_2} \text{sgn}(s)/c$ for $|s(t)| > L_s$. If the constants λ , M_s , and c are designed such that the inequality

$$\lambda \frac{M_s^{p_1/p_2}}{c} > x_{2m}$$

is satisfied, then it can be ensured that $x_2(t)$ does not re-enter \mathcal{R}_3 until $x_2(t) \in \mathcal{R}_2$.

Lemma 7 shows that when sliding mode occurs before $x_2(t)$ enters \mathcal{R}_2 , then the sliding mode continues to occur as $x(t) \in \mathcal{R}_2$. One possible trajectory of $x(t)$ is that $x(t)$ starts in \mathcal{Q}_1 , enters and exits \mathcal{R}_3 to the set $\{\mathcal{Q}_4 \setminus \mathcal{R}_3\}$, travels with an average constant velocity of $x_{2avg} = -\lambda M_s^{p_1/p_2} \text{sgn}(s)/c$, then enters \mathcal{R}_2 and converges to the origin as shown in Figure 3. Similarly, if $x(0)$ starts in \mathcal{Q}_3 , it enters and exits \mathcal{R}_3 to the set $\{\mathcal{Q}_2 \setminus \mathcal{R}_3\}$, travels with an average constant velocity of $x_{2avg} = -\lambda M_s^{p_1/p_2} \text{sgn}(s)/c$, then enters \mathcal{R}_2 and converges to the origin.

Theorem 1: For the system modeled in (1), where the sign of the uncertain input gain $b(x, t)$ is unknown, the control input $u(t)$ in (14)-(17) ensures that the surface $\tilde{s}(t)$ is reached

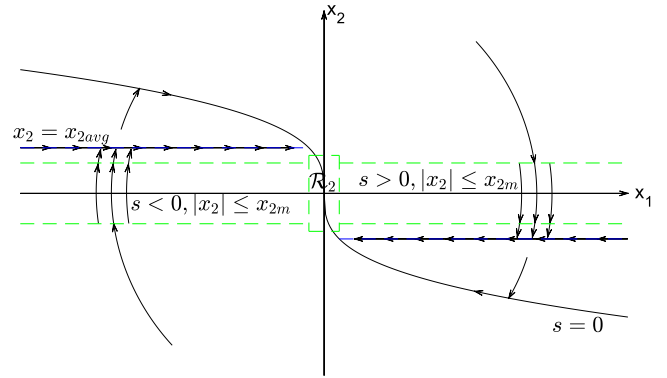


FIGURE 3. The phase plot of the system showing the trajectories of the system starting in $\mathcal{Q}_1 \cap \mathcal{R}_4$ and $\mathcal{Q}_3 \cap \mathcal{R}_4$ and converging to the origin in \mathcal{R}_2 .

in finite time, $s(t)$ reaches zero in finite time, and the state $x(t)$ reaches the origin in finite time.

Proof: Consider the multi-equilibrium Lyapunov candidate function

$$V = \left| \sin \frac{\pi \tilde{s}}{\varepsilon} \right| \quad (22)$$

Taking the time derivative along (1),

$$\dot{V} = \frac{\pi}{\varepsilon} \Psi \left(\cos \frac{\pi \tilde{s}}{\varepsilon} \right) \dot{\tilde{s}} \quad (23)$$

where $\dot{\tilde{s}}$ is expressed in (7). From (23), it is obvious that when $|g(x_2)b(x, t)u(t)|$ dominates in (10)-(13), the Lyapunov derivative in (23) becomes

$$\dot{V} = \frac{\pi}{\varepsilon} \left(\cos \frac{\pi \tilde{s}}{\varepsilon} \right) \dot{\tilde{s}} |\text{sgn}(b)| \quad (24)$$

Based on Lemma 3-7, $x_2(t)$ crosses the boundary layer $|x_2| \leq x_{2m}$ in (9), and the sign of Ψ_s is dominant everywhere except in the non-attractive set \mathcal{R}_1 . This implies that $\Psi \dot{\tilde{s}}$ is sign definite for some of the points. When $\cos \frac{\pi \tilde{s}}{\varepsilon}$ is ± 1 and $V = 0$, every other point guarantees that $\dot{V} < 0$. Thus, $V(t) \rightarrow 0$ in finite time, $\tilde{s}(t) \rightarrow \beta \in \mathbb{R}$ in finite time in (24), $s(t) \rightarrow 0$ in finite time in (5), and $(x_1, x_2) \rightarrow (0, 0)$ in finite time in (4).

A more detailed proof of finite time analysis is similar to [6] and [27] and is omitted here for brevity. ■

The lemmas above have been provided to prove that the control input $u(t)$ dominates in (10)-(13), and they are used in Theorem 1 to prove stability. These lemmas have been used to prove three main parts. The first part considers where $(x_1, x_2) \in \mathcal{R}_4$ is outside the neighborhood of the line $x_2(t) = 0$ in Lemma 3-4. It is shown that outside this region, the control $u(t)$ dominates the disturbance and the extra terms that cannot be canceled due to the uncertainty in the scalar input. The second part considers when $(x_1, x_2) \in \mathcal{R}_1$ is near the line $x_2 = 0$ in Lemma 5. This analysis is similar to nonsingular terminal sliding mode control in [6], where it is shown that the line $x_2(t) = 0$ is not attractive. This analysis is crucial due to the fact that the term $x_2(t)$ multiplies the control input in the hyper sliding surface $\tilde{s}(t)$ in (7) and

the control becomes ineffective when $g(x_2 = 0) = 0$. It is shown that the state does cross the line $x_2(t) = 0$ and the set \mathcal{R}_1 is unattractive. The third part considers the case where (x_1, x_2) is near the origin in Lemma 7. Since the control input $u(t)$ is multiplied by the function $g(x_2)$ in (7) and $|x_2(t)|$ is decreasing as (x_1, x_2) approaches the origin, the magnitude of $g(x_2)b(x, t)u(t)$ decreases as well. It is shown that in the worst case scenario, the term $|s(t)|$ decreases faster than $|g(x_2)b(x, t)u(t)|$, which allows sliding mode and the state (x_1, x_2) to reach and remain at the origin in finite time.

Lemma 6 shows the effect of convergence rate due to the added term $e^{c_2 x_2^2/2}$ on the surface $s(t)$ in (2). The term $e^{c_2 x_2^2/2}$ effectively magnifies the control input $u(t)$ via $g(x_2)$ in (4) to dominate cx_2 without increasing $u(t)$. However, this comes at the cost of restricting the upper limit on the velocity $x_2(t)$ as it approaches the origin.

Remark 2: The control gain selection is based on the user performance requirement. Control parameters such as M_1, M_2, M_3, M_4 are chosen based on the inequalities in (26), $M_2 \underline{b} > \bar{f}$, (21), and (47), respectively. To make the system converge faster, there are several variables that can be tuned. The constants c, M_s and λ can be increased to make $s(t)$ go to zero faster as $\tilde{s}(t)$ approaches a constant. This comes with a cost of increasing the control gain to dominate the increased magnitude in the extra terms. The variable ε can also be decreased to improve convergence time. Due to the fact that $s(t)$ is designed with the term $e^{c_2 x_2^2/2}$ that acts similar to the saturation function, there is performance trade off in the speed of convergence and control magnitude.

VI. SIMULATION RESULTS

Simulation results are presented for a second order system given in (1). The simulation parameters were chosen to be

$M_1 = 1$	$M_2 = .25$	$M_3 = .26$
$M_4 = 2.76$	$L_s = 1$	$M_s = .25$
$m_1 = 3$	$p_1 = 3$	$q_1 = 0.8$
$m_2 = 5$	$p_2 = 5$	$q_2 = 5.0$
$\lambda = 7$	$c = 2$	$d = 0.1$
$c_2 = 1$	$\varepsilon = 3.$	

The uncertain input scalar

$$b(x, t) = \cos(t) + \sin(x_1) \cos(x_2) + 4\text{sgn}(\sin(\frac{t}{2}))$$

was used in the simulation, but the controller development did not assume the knowledge of the sign of $b(x, t)$. The lower bound on $b(x, t)$ was considered to be $\underline{b} = 2$. The unknown non-vanishing disturbance $f(x, t)$ was considered as

$$f(x, t) = x_2 \cos(x_1) + 0.5 \sin(t).$$

The initial conditions were chosen to be

$$x_1(0) = -4 \quad x_2(0) = -1.5.$$

Figure 4 shows the time-varying position $x_1(t)$ and velocity $x_2(t)$, Figure 5 shows the time-varying hypersurface $\tilde{s}(t)$

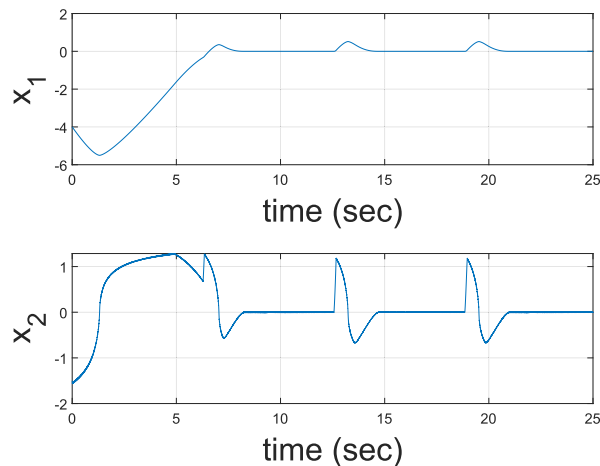


FIGURE 4. Plot of the time-varying position $x_1(t)$ and velocity $x_2(t)$. $x_1(t) \rightarrow 0$ and $x_2(t) \rightarrow 0$ in finite time.

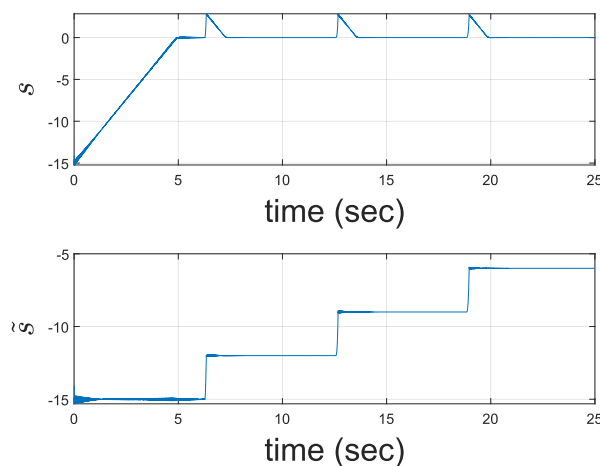


FIGURE 5. Plot of the hypersurface $\tilde{s}(t)$ and surface $s(t)$. $\tilde{s}(t) \rightarrow \beta$ and remains constant and $s(t) \rightarrow 0$.

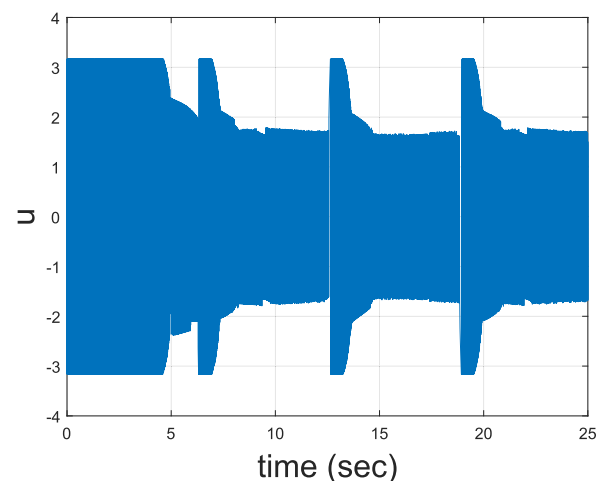


FIGURE 6. Plot of the control input $u(t)$ remains bounded at all times.

and surface $s(t)$, and Figure 6 shows the control input $u(t)$. In Figure 5, it can be seen that $\tilde{s}(t) = -15$ after a brief moment of time. This implies that the control direction $b(x, t)$

has been identified, and the system in (1) is sliding on $\tilde{s}(t) = -15$. This causes the surface $s(t)$ to approach zero and $s(5 < t < 6) = 0$. Note that the sliding surface reaches $s(t = 5) = 0$ before $(x_1, x_2) = (0, 0)$.

In Figure 4, it can be seen that $x(t)$ begins in \mathcal{Q}_3 since $\text{sgn}(x_1(0)) = \text{sgn}(x_2(0)) = -1$. The velocity $x_2(t)$ decreases into \mathcal{R}_3 and leaves \mathcal{R}_3 between $t = 1$ sec and $t = 2$ sec. As a result, $x(t)$ enters \mathcal{Q}_2 , and the velocity of x_2 approaches an average velocity until it reaches the set \mathcal{R}_2 . Around $t = 2\pi$, the sign of $b(x, t)$ changes, and $\tilde{s}(t)$ attaches itself to a new manifold $\tilde{s}(t) = -12$. Consequently, $s(t) \rightarrow 0$, and $(x_1, x_2) \rightarrow (0, 0)$ in finite time. Around $t = 4\pi$, the sign of $b(x, t)$ changes and the pattern repeats again. The control input remains bounded at all times while the sign of the scalar input changes in time.

VII. CONCLUSION

This paper presents a nonsingular terminal sliding mode controller for a second order system without *a priori* knowledge of the control direction and in the presence unknown non-vanishing state-dependent disturbances. The proposed approach achieves finite time convergence, and ensures that the control signals remain bounded at all times. Simulation results are provided to show the efficacy of the developed controller. Since the current method is developed for second order systems, future research will consider extending the current approach to higher order systems.

APPENDIX A PROOF OF LEMMA 3

Substituting (14) into (10) and using $\Psi_s = \text{sgn}(b\Psi)$ yields

$$P_1(x) = g|b|M_1\Psi_s + cx_2. \quad (25)$$

Consider the positive semi-definite function $g(x)$ in (6), where $e^{c_2x_2^2/2} \geq 1 \forall x_2(t)$. Also, it can be shown that $x_2^{(m_2+m_1)/m_1} \geq x_2$ for $|x_2| \geq 1$ and $x_2^{(m_2-m_1)/m_1} \geq x_2$ for $|x_2| \leq 1$. Therefore, M_1 can be chosen as

$$M_1 > \max\left(\frac{c}{c_2\underline{b}}, \frac{cm_1}{m_2\underline{b}}\right) \quad (26)$$

to ensure that $M_1c_2 > c$ and $M_1m_2/m_1 > c$. In (26), the fact that $\underline{b} \leq |b|$ is used. It follows from (25) and (26) that the sign of Ψ_s is dominant in (25) for $x_2(t) \in \mathbb{R}$.

Substituting (15) into (11), $P_2(x)$ can be obtained as $P_2 = g(f + |b|M_2\Psi_s)$. Since $g(x) \geq 0$, M_2 can be designed following the inequality $|M_2\underline{b}| > \underline{f}$ to ensure that the sign of Ψ_s dominates in $P_2(x)$, where $|f(x, t)| \leq \underline{f}$ and $\underline{b} \leq b$ are used.

Thus, the control inputs in (14) and (15) guarantee that the sign of Ψ_s dominates in (10) and (11).

APPENDIX B PROOF OF LEMMA 4

Substituting (16) into (12) and, using $\Psi_s = \text{sgn}(b\Psi)$, yields

$$P_3(x) = |\sigma(s)|^{p_1/p_2}g|b|M_3\Psi_s + \lambda\sigma^{p_1/p_2}(s). \quad (27)$$

In (6), $e^{c_2x_2^2/2} > 1 \forall x_2(t) \neq 0$. Therefore, using the set definition in (19) and (20), it is clear that $|\sigma(s)|^{p_1/p_2}g|bM_3| > |\lambda\sigma^{p_1/p_2}(s)|$ for $|x_2(t)| \geq x_{2m}$ in (27). Thus, the sign of Ψ_s dominates in (12).

APPENDIX C PROOF OF LEMMA 5

Without loss of generality, let $x(t) \in \mathcal{Q}_1$, i.e., $s(t)$ is positive. At any $t = t_0$, $x_2(t)$ is in $\mathcal{Q}_1 \cap \mathcal{R}_3$, i.e., $0 < x_2(t) \leq x_{2m}$, and, according to Lemma 3-4, $(M_1 + M_2)\Psi_s$ is sign dominant in (4). Therefore, using (1), the expression in (5) can be rewritten as

$$\text{sgn}(\dot{x}_2) = \Psi_s \quad (28)$$

$$\dot{\tilde{s}} = |\dot{s}| \Psi_s + \lambda\sigma^{p_1/p_2}(s). \quad (29)$$

Let $x_2(t)$ enter the boundary of \mathcal{R}_3 with $\Psi_s = -1$ and $|\dot{s}| < \lambda\sigma^{p_1/p_2}(s)$ in (29), such that the sliding mode does not continue to occur. From (28) and the facts that $x_1(t) > 0$ and $\Psi_s = -1$, it can be concluded that $x(t)$ moves towards \mathcal{Q}_4 .

Since the term $|\dot{s}| \Psi_s$ is dominated by $\lambda\sigma^{p_1/p_2}(s) > 0$, $\tilde{s}(t)$ goes from $\tilde{s}(t) = \beta$ to $\tilde{s}(t) = \beta + \varepsilon$ (see Figure 2) with the maximum rate of

$$\dot{\tilde{s}} = \lambda M_s^{p_1/p_2}$$

where $\dot{s} = 0$ is used to obtain the maximum rate of change of $\tilde{s}(t)$. When $\tilde{s}(t)$ goes from $\tilde{s}(t) = \beta$ to $\tilde{s}(t) = \beta + \varepsilon$, $\Psi_s = -1$ switches to $\Psi_s = +1$. If this switching occurs while $x_2 \in \mathcal{R}_3$ then $x_2(t)$ could remain in \mathcal{R}_3 because the average acceleration could be zero or positive, the sliding mode does not occur, and $x(t)$ does not converge to the origin. Consider the conservative scenario where $\tilde{s}(t)$ switches from $\tilde{s}(t_0) = \beta + \varepsilon/2$ to $\tilde{s}(t_{\tilde{s}}) = \beta + \varepsilon$. The minimum time $t_{\tilde{s}} \in \mathbb{R}$ in which $\tilde{s}(t)$ changes from $\beta + \varepsilon/2$ to $\beta + \varepsilon$, i.e., $\Psi_s(\tilde{s})$ switches in sign, can be obtained from (29) as

$$t_{\tilde{s}} = \frac{\varepsilon}{2M_s^{p_1/p_2}} - \varepsilon_{\tilde{s}} \quad (30)$$

where the average acceleration $\ddot{\tilde{s}}(t)$ is considered zero, and $\varepsilon_{\tilde{s}}$, defined in (21), has a known upper bound $\varepsilon_{\tilde{s}} \in \mathbb{R}^+$ that offsets for the chattering region along the manifold $\tilde{s}(t) = \beta$.

To prevent the sign switching from occurring within \mathcal{R}_3 , the velocity $x_2(t)$ has to cross the boundary from $x_2(t_0) = x_{2m}$ to $x_2(t_{x_2}) = -x_{2m}$ before Ψ_s changes in sign, which implies that the velocity has to exit the set \mathcal{R}_3 with a time interval less than $t_{\tilde{s}}$. To obtain the time required for $x_2(t)$ to travel from x_{2m} to $-x_{2m}$, consider the worst case scenario where $x_2(t)$ reduces with minimum acceleration $\dot{x}_2(t)$ due to contribution of $u_2(t)$ and $u_3(t)$ alone in (1) and $u_2(t)$ is designed to compensate for $f(t)$. The minimum acceleration $\dot{x}_2(t)$ can then be obtained as

$$\dot{x}_2 = \underline{b}M_s^{p_1/p_2}M_3\Psi_s \quad (31)$$

where $\underline{b} \leq |b|$ is used. Given the minimal acceleration in (31), the maximum time interval to leave the set \mathcal{R}_3 can be given by

$$t_{x_2} = \frac{2x_{2m}}{\underline{b}M_s^{p_1/p_2}M_3}. \quad (32)$$

Comparing (30) and (32), the control gain M_3 can be designed as in (21) to guarantee $t_{\tilde{s}} > t_{x_2}$, i.e., $x_2(t)$ will exit \mathcal{R}_3 and enter \mathcal{R}_4 before $\Psi_s(t)$ switches from -1 to $+1$. In $x(t) \in \mathcal{Q}_4$ and $x_2(t) \in \mathcal{R}_4$, according to Lemmas 3 and 4 and the fact that $t_{\tilde{s}} > t_{x_2}$, $x(t)$ remains attractive to the same manifold $\tilde{s}(t) = \beta$ that it was before entering \mathcal{R}_3 . When $x_2(t) \in \mathcal{R}_3$, $\tilde{s}(t)$ increases from β to $\beta + \varepsilon_2$, where $\varepsilon_2 < \varepsilon \in \mathbb{R}^+$. Consequently, sliding mode does not occur immediately after $x_2(t)$ exits \mathcal{R}_3 , and the velocity $x_2(t)$ continues to increase in magnitude.

When $x(t) \in \mathcal{Q}_3$, the analysis is similar to above, and hence is omitted for brevity. In this case, $\text{sgn}(s(t)) = -1$ and $x_2(t)$ crosses the boundary from $-x_{2m}$ to x_{2m} . As opposed to the case above where the surface $\tilde{s}(t)$ increases from β to $\beta + \varepsilon_2$ when $x_2(t)$ crosses \mathcal{R}_3 from \mathcal{Q}_1 to \mathcal{Q}_4 , in this case $\tilde{s}(t)$ decreases from β to $\beta - \varepsilon_2$ when $x_2(t)$ crosses \mathcal{R}_3 from \mathcal{Q}_3 to \mathcal{Q}_2 . It can be shown that, when the inequality in (21) is satisfied, the gain M_3 ensures that \mathcal{R}_3 for $|s(t)| > L_s$, i.e., \mathcal{R}_1 is not an attractive set.

**APPENDIX D
PROOF OF LEMMA 6**

When sliding mode occurs on $\tilde{s}(t) = \beta$, $\dot{\tilde{s}}(t) = 0$. Therefore, the expressions in (4) and (5) yield

$$g\dot{x}_2 + cx_2 = -\lambda\sigma^{p_1/p_2}(s).$$

Using the fact that $|s(t)| > L_s$, the acceleration $\dot{x}_2(t)$ can be obtained as

$$\dot{x}_2 = \frac{-cx_2 - \lambda M_s^{p_1/p_2} \text{sgn}(s)}{g}. \tag{33}$$

As $|x_2(t)|$ decreases or increases, depending on whether $x(t) \in \mathcal{Q}_2$ or $x(t) \in \mathcal{Q}_4$, respectively, and $x_1(t)$ approaches the origin, there exists a moment when $cx_2 = -\lambda M_s^{p_1/p_2} \text{sgn}(s)$ such that $\dot{x}_2(t) = 0$. Since $\dot{x}_2(t) = 0$ also satisfies $\dot{\tilde{s}}(t) = 0$, $x_1(t)$ approaches the origin with a constant speed of $\lambda M_s^{p_1/p_2} / c$ until $x_2(t)$ enters \mathcal{R}_2 .

**APPENDIX E
PROOF OF LEMMA 7**

Lemmas 3-5 guarantee that the sign of the terms containing Ψ_s dominate the closed-loop dynamics in (18) such that sliding mode occurs on $\tilde{s}(t) = \beta$. When $x_2(t)$ enters \mathcal{R}_2 , the inequality $|x_2(t)| \geq x_{2m}$ in Lemma 4 is not satisfied. However, within \mathcal{R}_2 , a more relaxed condition can be established by analyzing the control input $u_4(t)$ in (17) with the term $\lambda\sigma^{p_1/p_2}(s)$ in (12) to ensure that the sign of Ψ_s dominates in (7).

Let $P_5(x) = P_3(x) + P_4(x)$ and consider the contribution of control input $u_4(t)$ alone. Note that $\text{sgn}(u_3) = \text{sgn}(u_4) = \Psi$. Using (6), (12), (13), and (17), $P_5(x)$ can be obtained as

$$\begin{aligned} P_5(x) &= |\sigma(s)|^{q_1/q_2} e^{c_2 x_2^2/2} x_2^{(m_2-m_1)/m_1} |b| M_4 \Psi_s \\ &+ \frac{m_1}{m_2} |\sigma(s)|^{q_1/q_2} e^{c_2 x_2^2/2} c_2 x_2^{(m_1+m_2)/m_1} |b| M_4 \Psi_s \\ &+ \lambda \sigma^{p_1/p_2}(s). \end{aligned} \tag{34}$$

To maintain the sign dominance of $\Psi_s(\tilde{s})$ in (34), the following inequality must be satisfied:

$$\begin{aligned} &\underline{b} M_4 |\sigma(s)|^{q_1/q_2} e^{c_2 x_2^2/2} x_2^{(m_2-m_1)/m_1} \\ &+ \underline{b} M_4 \frac{m_1}{m_2} |\sigma(s)|^{q_1/q_2} e^{c_2 x_2^2/2} c_2 x_2^{(m_1+m_2)/m_1} \\ &\geq |\lambda \sigma^{p_1/p_2}(s)| \end{aligned} \tag{35}$$

where $\underline{b} \leq |b|$ is used. Since both the terms on the left in (35) are positive semi-definite, a conservative condition for the sign dominance of $\Psi_s(\tilde{s})$ can be obtained as

$$\underline{b} M_4 x_2^{(m_2-m_1)/m_1} \geq \left| \lambda \frac{\sigma^{p_1/p_2}(s)}{|\sigma(s)|^{q_1/q_2}} \right| \tag{36}$$

In (36), the fact that $e^{c_2 x_2^2/2} \geq 1$ is used.

In order for the sliding mode to continue to occur in \mathcal{R}_2 , the inequality in (36) must be satisfied at all times, which can be assured if (36) is satisfied at the initial time when $x_2(t)$ enters \mathcal{R}_2 and $s(t)$ converges to zero faster than $x_2(t)$ goes to the origin.

To simplify the subsequent analysis, the constants q_1 and q_2 in (17) are designed as

$$\begin{aligned} d &= \frac{p_2}{p_2 - p_1} \left(\frac{p_1}{p_2} - \frac{q_1}{q_2} \right) - 1 \\ \frac{q_1}{q_2} &= \frac{p_1 - (1+d)(p_2 - p_1)}{p_2} \end{aligned} \tag{37}$$

where $0 < q_1/q_2 < 1$, $0 < d < 1$, and $q_1/q_2 < p_1/p_2$.

Without loss of generality, let t_0 be the time when sliding mode occurs, i.e., $x(t)$ slides on a constant manifold $\tilde{s}(t) = \beta$. Using (5), $\dot{s} = -\lambda s^{p_1/p_2}$, where the fact that, in \mathcal{R}_2 , $|s(t)| \leq L_s$ or $\sigma(s) = s(t)$ is used. The solution of the differential equation for $\dot{s}(t)$ can be obtained as

$$s^{(p_2-p_1)/p_2}(t) = -\frac{p_2 - p_1}{p_2} \lambda t + s^{(p_2-p_1)/p_2}(t_0). \tag{38}$$

From (38), since $s^{(p_2-p_1)/p_2}(t) > 0$ everywhere except $s(t) = 0$, $s(t)$ goes to zero in finite time t_s given by

$$t_s = \frac{p_2 s^{(p_2-p_1)/p_2}(t_0)}{\lambda(p_2 - p_1)}. \tag{39}$$

When $s(t) = 0$, $x(t)$ approaches the origin and, for some $t_{x_1} > t_0$, $x_1(t_{x_1}) = x_2(t_{x_1}) = 0$ as shown in Figure 3. The velocity $x_2(t)$ with which $x_1(t)$ decays can be obtained by substituting $s(t) = 0$ in (2) as

$$x_2^{m_2/m_1} = \dot{x}_1^{m_2/m_1} = -\frac{cx_1}{e^{c_2 x_2^2/2}}. \tag{40}$$

In the following analysis, an expression for t_{x_1} is obtained and compared with (39) to obtain necessary gain conditions to ensure that $s(t)$ goes to zero faster than $x_2(t)$ or $x_1(t)$ goes to the origin. In (40), $e^{c_2 x_2^2/2} \geq 1 \forall x_2(t)$. Therefore, the largest decay rate of $x_1(t)$ can be obtained by considering $e^{c_2 x_2^2/2} = 1$ as $\dot{x}_1 = (-cx_1)^{m_1/m_2}$. The solution of the differential equation for $\dot{x}_1(t)$ can be obtained as

$$x_1^{(m_2-m_1)/m_2} = -\frac{m_2 - m_1}{m_2} c_1 t + x_1^{(m_2-m_1)/m_2}(t_0) \tag{41}$$

where $c_1 = c^{m_1/m_2} \in \mathbb{R}^+$. Using the fact that $x_1^{(m_2-m_1)/m_2} > 0$ everywhere except $x_1(t) = 0$, the time required for $x(t) \rightarrow 0$ once $s(t) = 0$ can be given as

$$t_{x_1} = \frac{m_2 x_1^{(m_2-m_1)/m_2}(t_0)}{c_1(m_2 - m_1)}. \quad (42)$$

The total estimated time t_x for $x(t) \rightarrow 0$ is the sum of the time required for $s(t) \rightarrow 0$ and the time required for $x(t) \rightarrow 0$ on $s(t) = 0$, i.e., $t_x = t_{x_1} + t_s$.

In general, when sliding mode occurs in $\tilde{s}(t) = \beta$, the surface $s(t) \rightarrow 0$, and then $(x_1, x_2) \rightarrow 0$ in a cascading manner, as shown above. This generally implies that $s(t) = 0$ before (x_1, x_2) reaches the origin. Since $s(t) = 0$ before $(x_1, x_2) \rightarrow 0$, the term $\lambda \sigma^{p_1/p_2}(s)$ in (7) vanishes, and no further analysis is necessary since $g(x_2)bu(t)$ is dominating.

In the worst case scenario when $s(t) \neq 0$ as $x(t) \rightarrow 0$, the surface $s(t)$ needs to be designed such that when $x(t) \in \mathcal{R}_2$, the magnitude of $s(t)$ decays faster than the magnitude of $g(x_2)bu(t)$ to guarantee the occurrence of sliding mode. Hence, the following analysis considers the worst case scenario that assumes $g(x_2)$ decays as fast as possible by letting $x_2(t)$ decay as fast as possible, while taking in the slowest decay of the magnitude of $s(t)$ by setting the time that $s(t_s) = x(t_x) = 0$, i.e., $t_x = t_s$.

Let $x(t)$ slide on $\tilde{s}(t) = \beta$ such that $|s(t)| \leq L_s$ and $s(t) \neq 0$, and consider the limiting case when $s(t)$ approaches zero at the same time that $x(t)$ approaches the origin, i.e., $t_x = t_s$. Using (39) and (42), $t_x = t_s$ implies that the initial conditions $s(0)$ and $x_1(0)$ can be related as

$$\frac{p_2 s^{(p_2-p_1)/p_2}(t_0)}{p_2 - p_1} = \frac{m_2 \lambda}{c_1(m_2 - m_1)} x_1^{(m_2-m_1)/m_2}(t_0). \quad (43)$$

Substituting (41) into $\dot{x}_1 = x_2 = (-cx_1)^{m_1/m_2}$ yields

$$x_2^{(m_2-m_1)/m_1} = -c_3 \left(-\frac{m_2-m_1}{m_2} c_1 t + x_1^{(m_2-m_1)/m_2}(t_0) \right) \quad (44)$$

where $c_3 = (-c)^{(m_2-m_1)/m_1} > 0$.

Substituting (37), (38), (43), and (44) into (36) yields a time and state dependent inequality that can be written as

$$c_3 \underline{b} M_4 \zeta \geq \lambda \zeta^{d+1} \quad (45)$$

where the positive semi-definite function $\zeta(t)$ is defined as

$$\zeta \triangleq \begin{cases} -\frac{c_1(m_2 - m_1)}{m_2} t + x_1^{(m_2-m_1)/m_2}(t_0) & \forall t_0 \leq t < t_s \\ 0 & \forall t_s \leq t \end{cases}$$

where $\zeta = 0 \forall t_s \leq t$ since $s(t_s) = x(t_x) = 0$ and $t_s = t_x$. For simplicity, designing $c_1 = \lambda$, $p_1 = m_1$, $p_2 = m_2$. Using (43) and the fact that $|s(t)| \leq L_s$ or $|\sigma(s)| \leq M_s$, $\zeta(t)$ can be upper bounded by a known constant $\zeta(t) < \bar{\zeta} \in \mathbb{R}^+$. The inequality in (45) can then be written as

$$c_3 \underline{b} M_4 > \lambda \bar{\zeta}^d \quad (46)$$

where the gain M_4 is chosen such that

$$M_4 > \frac{\lambda}{\underline{b} c_3} \bar{\zeta}^d. \quad (47)$$

Thus, by selecting M_4 based on (47), inequality (46) is satisfied and $s(t) \rightarrow 0$ faster than $x(t) \rightarrow 0$ thus guaranteeing that the sliding mode continues to occur in \mathcal{R}_2 .

REFERENCES

- [1] V. Utkin, "Variable structure systems with sliding modes," *IEEE Trans. Autom. Control*, vol. AC-22, no. 2, pp. 212–222, Apr. 1977.
- [2] S. T. Venkataraman and S. Gulati, "Control of nonlinear systems using terminal sliding modes," *J. Dyn. Syst., Meas., Control*, vol. 115, no. 3, pp. 554–560, Sep. 1993.
- [3] M. Zhihong and X. H. Yu, "Terminal sliding mode control of MIMO linear systems," *IEEE Trans. Circuits Syst. I, Fundam. Theory Appl.*, vol. 44, no. 11, pp. 1065–1070, Nov. 1997.
- [4] Y. Wu, X. Yu, and Z. Man, "Terminal sliding mode control design for uncertain dynamic systems," *Syst. Control Lett.*, vol. 34, no. 5, pp. 281–287, Jul. 1998.
- [5] Y. Feng, X. Yu, and F. Han, "On nonsingular terminal sliding-mode control of nonlinear systems," *Automatica*, vol. 49, no. 6, pp. 1715–1722, Jun. 2013.
- [6] Y. Feng, X. Yu, and Z. Man, "Non-singular terminal sliding mode control of rigid manipulators," *Automatica*, vol. 38, no. 12, pp. 2159–2167, Dec. 2002.
- [7] W. Chen, X. Li, W. Ren, and C. Wen, "Adaptive consensus of multi-agent systems with unknown identical control directions based on a novel Nussbaum-type function," *IEEE Trans. Autom. Control*, vol. 59, no. 7, pp. 1887–1892, Jul. 2014.
- [8] Y. Xudong and J. Jingping, "Adaptive nonlinear design without a priori knowledge of control directions," *IEEE Trans. Autom. Control*, vol. 43, no. 11, pp. 1617–1621, Nov. 1998.
- [9] Z. Yang, S. C. P. Yam, L. K. Li, and Y. Wang, "Robust control for uncertain nonlinear systems with state-dependent control direction," *Int. J. Robust Nonlinear Control*, vol. 21, no. 1, pp. 106–118, Jan. 2011.
- [10] M. Yu, X. Ye, and D. Qi, "Robust adaptive repetitive learning control for a class of time-varying nonlinear systems with unknown control direction," *J. Control Theory Appl.*, vol. 11, no. 3, pp. 336–342, Aug. 2013, doi: 10.1007/s11768-013-1094-2.
- [11] J.-X. Xu and R. Yan, "Iterative learning control design without a priori knowledge of the control direction," *Automatica*, vol. 40, no. 10, pp. 1803–1809, Oct. 2004.
- [12] Y. Su, "Cooperative global output regulation of second-order nonlinear multi-agent systems with unknown control direction," *IEEE Trans. Autom. Control*, vol. 60, no. 12, pp. 3275–3280, Dec. 2015.
- [13] X. Bu, D. Wei, X. Wu, and J. Huang, "Guaranteeing preselected tracking quality for air-breathing hypersonic non-affine models with an unknown control direction via concise neural control," *J. Franklin Inst.*, vol. 353, no. 13, pp. 3207–3232, Sep. 2016.
- [14] J. C. Willems and G. Byrnes, "Global adaptive stabilization in the absence of information on the sign of the high frequency gain," in *Analysis and Optimization of Systems*. Berlin, Germany: Springer, 1984, pp. 49–57.
- [15] G. Bartolini, A. Ferrara, and L. Giacomini, "A switching controller for systems with hard uncertainties," *IEEE Trans. Circuits Syst. I, Fundam. Theory Appl.*, vol. 50, no. 8, pp. 984–990, Aug. 2003.
- [16] T. R. Oliveira, A. J. Peixoto, E. V. L. Nunes, and L. Hsu, "Control of uncertain nonlinear systems with arbitrary relative degree and unknown control direction using sliding modes," *Int. J. Adapt. Control Signal Process.*, vol. 21, nos. 8–9, pp. 692–707, 2007.
- [17] L. Yan, L. Hsu, R. R. Costa, and F. Lizarralde, "A variable structure model reference robust control without a prior knowledge of high frequency gain sign," *Automatica*, vol. 44, no. 4, pp. 1036–1044, Apr. 2008.
- [18] T. R. Oliveira, A. C. Leite, A. J. Peixoto, and L. Hsu, "Overcoming limitations of uncalibrated robotics visual servoing by means of sliding mode control and switching monitoring scheme," *Asian J. Control*, vol. 16, no. 3, pp. 752–764, May 2014.
- [19] A. Scheinker and M. Krstic, "Minimum-seeking for CLFs: Universal semiglobally stabilizing feedback under unknown control directions," *IEEE Trans. Autom. Control*, vol. 58, no. 5, pp. 1107–1122, May 2013.
- [20] Y. Li, S. Tong, and T. Li, "Observer-based adaptive fuzzy tracking control of MIMO stochastic nonlinear systems with unknown control directions and unknown dead zones," *IEEE Trans. Fuzzy Syst.*, vol. 23, no. 4, pp. 1228–1241, Aug. 2015.

- [21] C. Wang, C. Wen, and Y. Lin, "Adaptive actuator failure compensation for a class of nonlinear systems with unknown control direction," *IEEE Trans. Autom. Control*, vol. 62, no. 1, pp. 385–392, Jan. 2017.
- [22] Y.-J. Liu, Y. Gao, S. Tong, and C. L. P. Chen, "A unified approach to adaptive neural control for nonlinear discrete-time systems with nonlinear dead-zone input," *IEEE Trans. Neural Netw. Learn. Syst.*, vol. 27, no. 1, pp. 139–150, Jan. 2016.
- [23] J. Kaloust and Z. Qu, "Robust control design for nonlinear uncertain systems with an unknown time-varying control direction," *IEEE Trans. Autom. Control*, vol. 42, no. 3, pp. 393–399, Mar. 1997.
- [24] G. Bartolini, A. Pisano, and E. Usai, "On the second-order sliding mode control of nonlinear systems with uncertain control direction," *Automatica*, vol. 45, no. 12, pp. 2982–2985, Dec. 2009.
- [25] S. Drakunov, U. Ozguner, P. Dix, and B. Ashrafi, "ABS control using optimum search via sliding modes," *IEEE Trans. Control Syst. Technol.*, vol. 3, no. 1, pp. 79–85, Mar. 1995.
- [26] C. Ton, S. S. Mehta, and Z. Kan, "Nonsingular terminal sliding mode control with unknown control direction," in *Proc. Amer. Control Conf. (ACC)*, May 2017, pp. 3730–3734.
- [27] S. V. Drakunov, "Sliding mode control with multiple equilibrium manifolds," *J. Dyn. Syst., Meas., Control*, vol. 55, no. 1, pp. 101–108, Nov. 1994.
- [28] Y. Xudong and Z. Ding, "Robust tracking control of uncertain nonlinear systems with unknown control directions," *Syst. Control Lett.*, vol. 42, no. 1, pp. 1–10, Jan. 2001.
- [29] Y.-J. Liu and S. Tong, "Barrier Lyapunov functions for Nussbaum gain adaptive control of full state constrained nonlinear systems," *Automatica*, vol. 76, pp. 143–152, Feb. 2017.
- [30] C. Ton, S. S. Mehta, and Z. Kan, "Super-twisting control of double integrator systems with unknown constant control direction," *IEEE Control Syst. Lett.*, vol. 1, no. 2, pp. 370–375, Oct. 2017.
- [31] W. Chen, C. Wen, and J. Wu, "Global exponential/finite-time stability of nonlinear adaptive switching systems with applications in controlling systems with unknown control direction," *IEEE Trans. Autom. Control*, vol. 63, no. 8, pp. 2738–2744, Aug. 2018.
- [32] J. Wu, J. Li, G. Zong, and W. Chen, "Global finite-time adaptive stabilization of nonlinearly parametrized systems with multiple unknown control directions," *IEEE Trans. Syst., Man, Cybern. Syst.*, vol. 47, no. 7, pp. 1405–1414, Jul. 2017.
- [33] T. R. Oliveira, L. Hsu, and A. J. Peixoto, "Output-feedback global tracking for unknown control direction plants with application to extremum-seeking control," *Automatica*, vol. 47, no. 9, pp. 2029–2038, Sep. 2011.



DONGMEI LÜ is currently pursuing the Ph.D. degree in mechanical engineering from the Hefei University of Technology, Hefei, Anhui, China. Since 2016, she has been an Associate Professor with the Anhui Communications Vocational and Technical College. She has published dozens of teaching and research articles. Her research interests include numerical control technology and mechanical dynamic characteristics research. Her awards and honors include the Anhui Province Development Talent, Excellent Teaching Achievements Award, the First Prize of Teaching Achievements of Anhui Province, and the Teaching Masters of Anhui Province.

• • •